X-ray spectroscopy of high-temperature plasma

L. P. Presnyakov

P. N. Lebedev Physics Institute, USSR Academy of Sciences
Usp. Fiz. Nauk **119**, 49–73 (May 1976)

The review is devoted to the results and method of a theoretical investigation of x-ray spectra of multiply-charged ions, with the aid of which the main parameters of astrophysical and laboratory nonstationary plasma are investigated. A distinguishing freature of such spectra is the presence of characteristic lines—satellites—producedin radiative decay of autoionization states. Calculation methods are described, with which to identify reliably the spectra $\Delta\lambda/\lambda = 10^{-4}$ at $\lambda \approx 1$ Å. The principal mechanisms of satellite formation—dielectronic recombination and direct excitation of K shells, are considered. The development of modern theory of electron-ion collisions makes it possible to calculate the intensities of the spectral lines with accuracy not worse than several percent. A comparison of the calculated and observed relative intensities of the satellites makes it possible to determine the temperature and density of the electrons, multiplicity distribution of the ions in the active regions and in x-ray bursts on the sun, and also in the dense laboratory (laser, etc.) plasma. A number of solar and laboratory spectra are analyzed.

PACS numbers: 52.25.Ps, 52.20.Hv, 96.20.Fw

CONTENTS

1. INTRODUCTION

Spectroscopic research on hot astrophysical and laboratory plasma in the far ultraviolet and x-ray bands of the spectrum have intensively progressed during the last few years. The objects of study in this case are the spectra of multiply-charged ions. In the solar corona and in other astrophysical objects, the concentration of the heavy elements are small fractions of one percent, and the plasma density does not exceed 10^{11} cm^{-3}.

A laboratory plasma can be chemically homogeneous, and its density can be comparable with the density of a solid. In such a wide range of parameters of the investigated objects, spectroscopic research methods are the most universal, and frequently (in the case of astrophysical plasma) the only feasible ones.

Qualitative conclusions concerning the presence of some particular element can be drawn even from the general structure of the spectrum, and the degree of ionization of the element characterizes the order of magnitude of the temperature of the investigated plasma. However, the present status of spectroscopic research of solar x-ray flares was initiated in experiments[1–4] in which the spectra of the helium-like and lithium-like iron ions Fe XXV–Fe XXIV were registered, on board the satellites "Interkosmos-4" and "Interkosmos-7", in the wavelength interval 1.85–1.95 Å with a resolution 5×10^{-4} Å. At the same time, systematic investigations were initiated of the spectra of the high-temperature plasma produced when high-power laser radiation is focused on a solid target.[5–12] These investigations have by now become quite widespread,[13–20] with other laboratory sources in use besides laser plasma.[21–24] The purpose of the research is not only the identification of the spectral lines (although up to the start of the 1970's the data on the spectra of ions with charges $Z > 10$ are exceedingly scanty), but also the establishment of the mechanism whereby the x-ray spectrum is excited, i.e., the determination of the physical parameters of the processes in the radiation source. By the same token, a vital task of the laboratory investigations is to reproduce a number of properties that are typical of active regions and flares on the sun, and in final analysis, the problem of simulating an astrophysical plasma under laboratory conditions.

This raises, naturally, the question of how much information can be gained from the line spectra registered in a limited wavelength interval, i.e., the extent to which their interpretation can be unambiguous. X-ray spectra of multiply-charged ions are characterized by an extraordinary abundance of lines, the greater part of which is connected with radiation decay of autoionization states, which are missing from the spectra of neutral atoms. Thus, the development of x-ray spectroscopy of hot plasma (astrophysical and laboratory) calls for the solution of the following problems:

1) Calculation of the wavelength and other spectroscopic characteristics of multiply-charged ions, with an accuracy that guarantees reliable identification of the experimental data.

2) Establishment of the mechanisms whereby the spectra are excited.

3) Development of diagnostic methods.

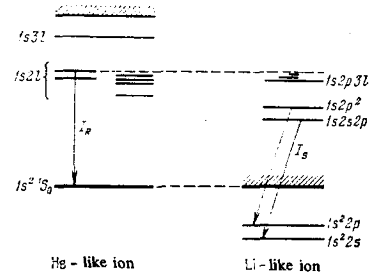

FIG. 1. Level scheme of helium- and lithium-like ions.

These questions can at present be given unambiguous answers by using the modern accomplishments of theoretical spectroscopy and of the physics of electron-ion collisions.

By the same token, the physics of high-temperature plasma gains a very effective research method applicable to a large group of vital problems. These include, for example, the study of the structure and the dynamics of the development of active regions and x-ray flares on the sun, which contribute to the understanding of the physical nature of these phenomena. It appears that it will be possible to obtain in the nearest future high-resolution spectra of astrophysical objects such as supernova remnants, and this will yield valuable information on their evolution. In laboratory experiments, the methods of x-ray spectroscopy are used to investigate very important characteristics of inhomogeneous and nonstationary plasma produced in installations for thermonuclear fusion and in other sources.

Under stationary conditions, the electron temperature of the plasma determines many other plasma parameters, in particular the distribution of the atoms with respect to the degrees of ionization. In a nonstationary plasma, which is realized in most cases in practice, the degree of ionization of the medium can be higher or lower than the level corresponding to a given electron temperature, depending on the initial conditions. It is therefore meaningful to determine, besides the electron temperature and the density, the degree of ionization of the medium, so as to establish the deviation for stationarity and ultimately investigate the dynamics of plasma development.

The general methods and results reported in this review are equally applicable to ions of any isoelectronic sequence. In the illustrations we shall confine ourselves predominantly, following[25–27], to the investigations of spectra of multiply-charged ions with two or three electrons. First, these ions are simple enough for a comprehensive theoretical analysis. Second, and more important, they contain enough information in that their spectra have been most thoroughly investigated under astrophysical and laboratory conditions.

2. SPECTRA OF MULTIPLY-CHARGED IONS

In their general structure, the spectra of multiply-charged ions duplicate the spectra of neutral atoms of the same isoelectronic sequence, being shifted into the short-wave band with increasing nuclear charge. However, in the spectrum of any source containing multiply-charged ions, each bounded spectral interval contains a large number of so-called satellites. Satellites are defined as lines produced from a state in which two or more electrons are excited. Let γ_0 be the set of quantum numbers characterizing the ground state of the ion, and let γ_1 coincide with the excited state. Then the satellite of the transition $\gamma_1 \to \gamma_0$ is defined as the transition $\gamma_1 nl \to \gamma_0 nl$ belonging to the ion having a multiplicity smaller by unity. In the case of a large nuclear charge, the presence of an additional electron nl leads only to an insignificant change of the wavelength in comparison with the $\gamma_1 \to \gamma_0$ transition. The foregoing is illustrated in Fig. 1, which shows the energy level scheme in helium-like and lithium-like ions with identical nuclear charge. Since the states $\gamma_1 nl$ are autoionization states, the satellite lines correspond to radiative decay of autoionization states. It follows therefore that their intensity increases with increasing charge of the nucleus. Indeed, the doubly-excited state of the ion A_Z (Z is the spectroscopic symbol of the ion) can decay via two channels:

radiation–$A_Z(\gamma_1 nl) \to A_Z(\gamma_0 nl) + \hbar\omega$,

or autoionization–$A_Z(\gamma_1 nl) \to A_{Z+1}(\gamma_0) + e$.

It is known that the autoionization probability depends little on the charge of the ion, whereas the probability of the radiative transition increases in proportion to Z^4 for dipole-allowed transitions.

The first weak optical transitions of the type

$$1s2pnl \to 1s^2nl \qquad (1)$$

(i.e., satellites on the lines $1s2p \to 1s^2$ of helium-like atoms) were first observed experimentally and identified in 1939 by Edlen and Tyren[28] in light-element spectra obtained with the aid of a vacuum spark. Subsequently, the state of the "usual transitions" was extended to include elements with nuclear charge $Z_n \lesssim 10$,[29–31] using installations of the "theta pinch" and "plasma focus" type. Investigations of the spectra of hotter sources, such as active regions and flares on the sun,[32–35] as well as of the plasma produced when high-power radiation is focused on a solid surface, have shown that the satellites in the spectra of high-charge ions ($Z_n > 10$) have an intensity comparable with the intensity of the resonance lines.

Among the satellites of type (1), the most intense and remote from the resonance line are the transitions with $n = 2$ (see Fig. 1), which are indeed those mainly investigated in spectroscopic research. Transitions with $n = 3$ are directly adjacent to the resonance line, and at $n \geqslant 4$ they are practically indistinguishable from the resonance line. Their combined intensity is small in comparison with the intensity of the resonance line. When the fine structure of the terms is taken into account, the total number of satellites corresponding to a transition from doubly excited states with principal quantum number $n = 2$ is quite large: even the resonance lines of H- and He-like ions have more than 20 long-wave satellites. This calls for a high degree of accuracy in the analysis of the energy terms of multiply-charged ions.

TABLE I. Wavelengths (Å), measured in the spectrum of a solar flare[1–4] and in a laboratory source,[24] and calculated within the framework of the Hartree–Fock,[26,27] and Coulomb[36–39] methods for helium- and lithium-like iron ions.

Measurement		Calculation		Arbitrary symbol
Refs. 1–4	Refs. 24	Refs. 26–27	Refs. 36–39	
1.8500	1.8500	1.8500	1.8499	w
1.8525	1.8520	1.8520	1.8520	n
1.8555	—	1.8551	1.8549	x
—	1.8560	1.8563	1.8563	m
1.8580	1.8579	1.8573	1.8574	b
1.8585	1.8589	1.8591	1.8589	y
1.8615	—	1.8616	1.8618	a
—	1.8620	1.8621	1.8624	d
1.863	1.8631	1.8633	1.8627	k
1.866	1.8655	1.8657	1.8655	j
1.868	—	1.8677	1.8678	z

When it comes to classifying and calculating the energy terms of multiply-charged ions, it is very important to take a correct account of the type of coupling between the angular and spin momenta of the electrons. We will recall that the LS coupling corresponds to smallness of the relativistic effects in comparison with the electrostatic effects, while the jj coupling is realized in the opposite limiting case. A situation wherein the electrostatic and relativistic effects are of the same order of magnitude and none of the simple types of coupling can be postulated is called intermediate coupling. Another important factor characteristic of many-electron systems is the effect of the correlational interaction between the electrons, which causes the many-electron wave functions to differ from the antisymmetrized combinations of single-electron functions. This effect can be taken into account by introducing an interaction (or a superposition) of configurations having the same principal quantum number.

At the present time systematic calculations, in which the indicated physical effects are taken into account, have already been performed on the spectra of multiply-charged ions, using two approaches: the Hartree–Fock approach[26,27] and the Coulomb expansion in the parameter Z^{-1}.[36–41]

The calculation of the terms (and consequently of the spectral lines) is carried out in the following manner. We write down the Hamiltonian of the system of N electrons in the field of a nucleus having a charge Z_n in the form

$$\mathcal{H} = \mathcal{H}_0 + \mathcal{H}', \tag{2}$$

where

$$\mathcal{H}_0 = \sum_{i=1}^{N} \left(-\frac{\hbar^2}{2m}\Delta_i - \frac{e^2 Z_n}{r_i} \right) + \sum_{i>j} \frac{e^2}{r_{ij}} \tag{3}$$

and $\mathcal{H}'$ contains relativistic (spin-orbit, etc.) terms. We denote the set of quantum numbers SLJ by the letter a, and write down in the zeroth approximation

$$\mathcal{H}_0 \varphi_n(a) = \varepsilon_n(a) \varphi_n(a), \quad a = \{SLJ\}, \tag{4}$$

$$\varphi_n(a) = \sum_p \prod_{i=1}^{N} C^n_{pi} \varphi_p(r_i); \tag{5}$$

Here $\varphi_p(r_i)$ are the single-electron wave functions, and the coefficients C^n_{pi} should be written down with allowance for the antisymmetrization and for the rules adding angular momenta in the LS-coupling scheme, which is the zeroth approximation. The transition from the zeroth Hamiltonian $\mathcal{H}_0(3)$ to the Hamiltonian (2) yields the states of the total Hamiltonian $\mathcal{H}$ defined as

$$\psi_n(\gamma) = \sum_{a'} V(a' \mid \gamma) \varphi_n(a'). \tag{6}$$

The coefficients $V(a|\gamma)$ are the eigenvectors of the transformation to the intermediate coupling, and are obtained by solving the secular equations:

$$\mathcal{H}_{\gamma\gamma'} - \delta_{\gamma\gamma'} E_\gamma = 0, \tag{7}$$

with

$$\mathcal{H}_{\gamma\gamma'} = \langle \gamma \mid \mathcal{H} \mid \gamma' \rangle = \sum_{a, a'} V(a \mid \gamma) V(a' \mid \gamma') \mathcal{H}_{aa'}, \tag{8}$$

$$\mathcal{H}_{aa'} = \langle a \mid \mathcal{H} \mid a' \rangle. \tag{9}$$

The eigenvalues E_γ yield the energy terms with allowance for the intermediate coupling and the correlation interaction (superposition of configurations). In accordance with the established tradition,[42,43] the terms E_γ are classified by using the quantum numbers SLJ, bearing in mind at the same time that they pertain not to the "pure" LS states, but to suitably mixed ones.

Within the framework of the Hartree–Fock approach,[26,27] the matrix elements (9) are calculated with the wave functions (5) obtained by numerically integrating Eq. (4) with account taken of the exchange potentials.

In the Coulomb approach,[36–39] the matrix elements (9) are calculated by using perturbation theory in terms of the small parameter Z^{-1} on the basis of hydrogen-like functions. The matrix elements can be represented in the form

$$\langle a \mid \mathcal{H} \mid a' \rangle = Z^2 \mathcal{H}^{(0)}_{aa'} + Z \mathcal{H}^{(1)}_{aa'} + \mathcal{H}^{(2)}_{aa'} + \ldots, \tag{10}$$

where the corrections $\mathcal{H}^{(1)}_{aa'}$, $\mathcal{H}^{(2)}_{aa'}$, ..., containing infinite sums over the discrete and continuous spectra, are calculated in closed analytic form.

In both methods, on going over to the intermediate coupling, account is taken of the same physical effects that are described in terms of different zeroth-approximation basis wave functions. The Coulomb approach is, in accordance with its structure, asymptotic in the parameter Z^{-1}. It has the advantage of universality. The Hartree–Fock method is applicable for all values of Z, but its use calls for numerical integration of the Schrödinger equation (4) for each value of Z.

The results of the calculation, within the framework of the methods described here, are compared with available experimental data in Table I, which lists the wave lengths of the resonance (w), intercombination (x, y) and "forbidden" (z) lines of the ion Fe XXV, and also a number of their satellites radiated by the Fe XXIV ion. To avoid the use of a cumbersome spectroscopic designation of the transitions, we use henceforth the arbitrary symbols[26,27] which have already gained wide popularity (Tables II and III). The presented data enable us to estimate the errors of the existing measure-

TABLE II. Arbitrary symbols for resonance lines of hydrogen-like ions and accompanying satellites.

Configurations	Multiplet	Line	Symbol	Configurations	Multiplet	Line	Symbol
$2s^2 \to 1s2p$	$^1S \to {}^1P$	$0 \to 1$	A			$2 \to 2$	Q
	$^1S \to {}^3P$	$0 \to 1$	B		$^1D \to {}^3P$	$2 \to 2$	R
$2p^2 \to 1s2p$	$^3P \to {}^1P$	$0 \to 1$	C	$2s2p \to 1s2s$	$^1P \to {}^1S$	$1 \to 0$	S
		$1 \to 1$	D		$^3P \to {}^1S$	$1 \to 0$	T
		$2 \to 1$	E		$^1P \to {}^3S$	$1 \to 1$	U
	$^1S \to {}^1P$	$0 \to 1$	F		$^3P \to {}^3S$	$0 \to 1$	V
	$^1D \to {}^1P$	$2 \to 1$	G			$1 \to 1$	X
	$^3P \to {}^3P$	$1 \to 0$	H			$2 \to 1$	Y
		$0 \to 1$	I				
		$1 \to 1$	K	$2p \to 1s$	$^2P \to {}^2S$	$\frac{3}{2} \to \frac{1}{2}$	L_{α_1}
		$2 \to 1$	M				
	$^1S \to {}^3P$	$0 \to 1$	N			$\frac{1}{2} \to \frac{1}{2}$	L_{α_2}
	$^1D \to {}^3P$	$2 \to 1$	O				
	$^3P \to {}^3P$	$1 \to 2$	P				

ments and calculations by means of $\Delta\lambda/\lambda \approx 10^{-4}$ for $\lambda \approx 1$–2 Å. This estimate characterizes simultaneously the degree of accuracy of each of the discussed calculation methods, since the zeroth-approximation basis in both cases is constructed on the basis of nonrelativistic wave functions.

The wavelengths of the resonance lines and satellites for a number of hydrogen-, helium-, and lithium-like ions are given in Tables IV and V. Much more detailed tables are given in[26,39]. Thus, the results of the corresponding calculations of the wavelengths guarantee the necessary accuracy for the identification of the experimental spectra. This circumstance is most important for the analysis of physical processes that lead to the formation of the spectra of multiply-charged ions.

3. MECHANISMS OF SPECTRUM EXCITATION

In a high-temperature plasma containing multiply-charged ions, the rates of excitation and ionization by electron impact greatly exceed the rates of the corresponding processes due to ion-ion interactions, the smallness of which is due to the Coulomb repulsion between the ions. At the same time, spontaneous decay of excited states—radiative transitions and autoionization—predominate over collision decays. This facilitates to a considerable degree the analysis of the distribution of the ions over the excited states and ultimately makes it possible to express the spectral-line intensities in the form of simple functions of the probabilities of the radiative decay of the excited states and the reaction rates of the electron-ion interactions.

TABLE III. Arbitrary symbols for resonance and intercombination lines of He-like ions and the accompanying satellites.[26–27]

Configurations	Multiplet	Line	Symbol	Configurations	Multiplet	Line	Symbol
$1s2p^2 \to 1s^22p$	$^2P \to {}^2P^0$	$\frac{3}{2} \to \frac{3}{2}$	a			$\frac{1}{2} \to \frac{1}{2}$	d
		$\frac{3}{2} \to \frac{1}{2}$	b		$^4P \to {}^2P^0$	$\frac{5}{2} \to \frac{3}{2}$	e
		$\frac{1}{2} \to \frac{3}{2}$	c			$\frac{3}{2} \to \frac{3}{2}$	f
		$\frac{3}{2} \leftarrow \frac{1}{2}$	g			$\frac{1}{2} \to \frac{1}{2}$	p
		$\frac{1}{2} \to \frac{3}{2}$	h	$1s2p2s \to 1s^22s$	$(^1P)^2P^0 \to {}^2S$	$\frac{3}{2} \to \frac{1}{2}$	q
		$\frac{1}{2} \to \frac{1}{2}$	i			$\frac{1}{2} \to \frac{1}{2}$	r
	$^2D \to {}^2P^0$	$\frac{5}{2} \to \frac{3}{2}$	j		$(^3P)^2P^0 \to {}^2S$	$\frac{3}{2} \to \frac{1}{2}$	s
		$\frac{3}{2} \to \frac{1}{2}$	k			$\frac{1}{2} \to \frac{1}{2}$	t
		$\frac{3}{2} \to \frac{3}{2}$	l		$^4P^0 \to {}^2S$	$\frac{3}{2} \to \frac{1}{2}$	u
	$^2S \to {}^2P^0$	$\frac{1}{2} \to \frac{3}{2}$	m			$\frac{1}{2} \to \frac{1}{2}$	v
		$\frac{1}{2} \to \frac{1}{2}$	n	$1s2p \to 1s^2$	$^1P^0 \to {}^1S$	$1 \to 0$	w
					$^3P^0 \to {}^1S$	$2 \to 0$	x
$1s2s^2 \to 1s^22p$	$^2S \to {}^2P^0$	$\frac{1}{2} \to \frac{3}{2}$	o			$1 \to 0$	y
				$1s2s \to 1s^2$	$^3S \to {}^1S$	$1 \to 0$	z

TABLE IV. Wavelengths (Å) of H- and He-like ions and intercombination lines of He-like ions.[39,27]

	Mg	Si	Ca	Fe	Ni	Cu
L_{α_1}	8.4174	6.1788	3.0172	1.7770	1.5293	1.4243
L_{α_2}	8.4228	6.1842	3.0226	1.7824	1.5347	1.4297
w	9.1678	6.6470	3.1765	1.8500	1.5880	1.4771
x	9.2280	6.6846	3.1887	1.8551	1.5919	1.4807
y	9.2314	6.6880	3.1924	1.8591	1.5961	1.4849
z	9.3135	6.7394	3.2103	1.8677	1.6031	1.4913

A. Excitation of ions by electron impact

The physical picture of elastic and inelastic scattering of an electron by an ion is more complicated and contains more information than scattering by a neutral atom. The Coulomb attraction leads to characteristic singularities—resonances in the effective cross sections near the thresholds of new (energywise closed)

TABLE V. Wavelengths λ (Å) of satellites, autoionization A_a (10^{13} sec^{-1}) and radiative A_r (10^{13} sec^{-1}) decay probabilities of doubly-excited states.

	Mg			Ca			Fe		
	λ	A_a	A_r	λ	A_a	A_r	λ	A_a	A_r
	Satellites of resonance lines of H-like ions[39]								
A	8.6680	34.4	0.508	3.0790	33.4	3.73	1.8104	31.8	10.5
B	8.6137	34.4	0.0002	3.0646	33.4	0.026	1.8019	31.8	0.229
C	8.5868	0.0142	0.0071	3.0600	0.182	1.04	1.8009	0.356	10.3
D	8.5850	0	0.001	3.0579	0	0.132	1.7983	0	1.20
E	8.5820	0.220	0.023	3.0554	4.26	3.28	1.7966	12.12	25.0
F	8.4441	1.788	1.89	3.0259	2.66	14.6	1.7824	3.90	35.6
G	8.5497	37.2	2.42	3.0476	33.0	31.8	1.7913	25.2	28.3
H	8.5311	0	0.813	3.0430	0	6.52	1.7893	0	19.0
I	8.5335	0.0153	2.43	3.0458	0.182	18.0	1.7924	0.358	42.3
K	8.5317	0	0.609	3.0437	0	4.75	1.7899	0	13.1
M	8.5287	0.220	0.598	3.0412	4.26	3.26	1.7882	12.12	2.95
N	8.3925	1.788	0.011	3.0120	2.66	1.54	1.7741	3.90	14.7
O	8.4969	37.2	0.157	3.0335	33.0	2.06	1.7830	25.2	15.2
P	8.5343	0	1.02	3.0470	0	8.12	1.7936	0	23.6
Q	8.5313	0.220	1.82	3.0445	4.26	13.0	1.7919	12.12	28.8
R	8.4994	37.2	0.001	3.0368	33.0	1.69	1.7867	25.2	14.0
S	8.4943	20.2	1.25	3.0359	20.2	9.84	1.7866	19.58	27.8
T	8.5983	1.37	0.0007	3.0609	1.55	0.097	1.7998	2.06	1.04
U	8.4208	20.2	0.00001	3.0188	20.2	0.01	1.7785	19.58	0.011
V	8.5240	1.36	1.22	3.0446	1.360	9.73	1.7925	1.36	28.3
X	8.5230	1.37	1.22	3.0435	1.55	9.65	1.7916	2.06	27.3
Y	8.5193	1.36	1.23	3.0397	1.36	9.78	1.7875	1.36	28.6
	Satellites of resonance lines of He-like ions[26,27]								
a	9.2956	0.073	2.54	3.2029	1.02	23.7	1.8616	2.55	69.3
b	9.2922	0.073	0.397	3.1988	1.02	1.75	1.8573	2.55	2.12
c	9.2988	0.01	0.939	3.2070	0.016	7.06	1.8664	0.036	17.6
d	9.2955	0.001	2.01	3.2030	0.016	19.3	1.8621	0.036	58.6
e	9.3825	0.016	0.001	3.2230	0.523	0.309	1.8721	2.57	4.27
f	9.3851	0.003	0.001	3.2254	0.049	0.092	1.8741	0.173	0.876
g	9.3817	0.003	0.00001	3.2212	0.049	0.003	1.8697	0.173	0.028
h	9.3867	0	0.00002	3.2273	0	0.003	1.8763	0.010	0.004
i	9.3833	0	0.0005	3.2231	0	0.114	1.8719	0.010	1.71
j	9.3213	12.3	0.975	3.2104	14.4	8.56	1.8657	13.5	22.6
k	9.3182	12.2	0.909	3.2073	13.9	10.1	1.8633	13.3	33.9
l	9.3215	12.2	0.079	3.2114	13.9	0.006	1.8677	13.3	2.00
m	9.2214	1.38	0.641	3.1895	1.79	7.31	1.8563	1.98	26.1
n	9.2181	1.38	0.253	3.1854	1.79	1.06	1.8520	1.98	0.978
o	9.5693	11.1	0.068	3.2616	13.0	0.556	1.8895	13.9	1.45
p	9.5658	11.1	0.036	3.2574	13.0	0.402	1.8850	13.9	1.75
q	9.2835	0.525	1.802	3.1998	0.192	17.0	1.8603	0.037	52.6
r	9.2856	0.813	1.720	3.2024	2.10	13.0	1.8633	3.90	29.5
s	9.2348	7.97	0.181	3.1909	9.90	0.807	1.8565	10.8	0.058
t	9.2359	7.69	0.260	3.1917	7.99	4.88	1.8571	6.92	24.0
u	9.3904	0.001	0.007	3.2246	0.013	0.137	1.8730	0.044	1.62
v	9.3920	0	0.0003	3.2261	0.009	0.057	1.8744	0.054	0.732

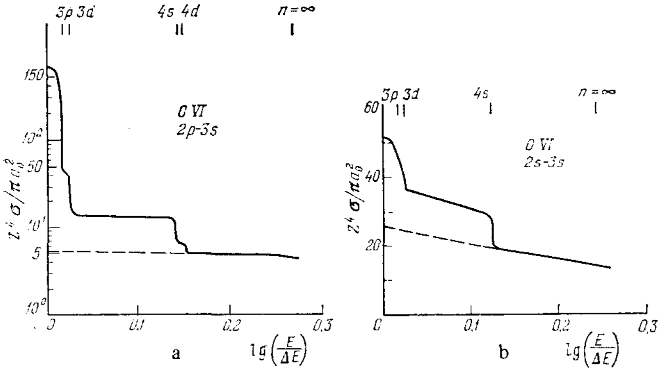

FIG. 2. Cross sections for the excitation of the transitions $1s^22p \to 1s^23s$ (a) and $1s^22s \to 1s^23s$ (b) in the O VI ion.[49,50] The dashed line indicates potential scattering.

channels, the cause of which is the formation and decay of quasistationary states of the ion-plus-electron system[44–49] (the so-called resonance scattering).

Resonance scattering can be qualitatively represented in the following manner. Each level γ of the ion A_Z is the limit of a sequence of levels γnl of the ion A_{Z-1} (with multiplicity smaller by unity), which converges to γ as $n \to \infty$. A characteristic example of such levels γnl (with $n=2$) is the doubly-excited state considered in Sec. 1. If the energy of the ion-plus-electron system coincides with the energy of the level γnl, then the result of the collision is the formation of a quasistationary state which decays radiatively or by autoionization. The autoionization decay with formation of an excited ion makes an additional contribution to the excitation cross section. Thus, besides the direct (or potential) excitation $\gamma_0 \to \gamma_1$

$$A_Z(\gamma_0) + e \to A_Z^*(\gamma_1) + e \tag{11a}$$

it is necessary to take into consideration the process of resonant excitation

$$A_Z(\gamma_0) + e \to A_{Z-1}^{**}(\gamma nl) \to A_Z^*(\gamma_1) + e, \tag{11b}$$

which adds to the effective cross section of the direct excitation a sequence of narrow resonances that converges to the threshold of the opening up of the new channel. It is known[45–49] that the resonant contribution averaged over a finite energy interval yields an energy-independent increment that vanishes jumpwise when a new channel is open. However, allowance for the radiative decay channel of the resonances, i.e., for the process

$$A_Z(\gamma_0) + e \to A_{Z-1}^{**}(\gamma nl) \to A_{Z-1} + \hbar\omega, \tag{12}$$

leads to a smoothing of the jumps in the immediate vicinity of the threshold.[49,50] It is important that in the region of the existence of the resonance scattering, i.e., at incident-electron energy values from the threshold of the excitation of the level γ_1 to the ionization potential of the ion A_Z, the contribution of the resonance scattering, generally speaking, is of the same order of magnitude as the direct excitation, and is in many cases decisive.

In the general case, the multichannel problem of excitation by electron impact is quite complicated. However, in the case of excitation of multiply-charged ions there arises in natural fashion a small parameter Z^{-1}, where $(Z-1)$ is the charge of the ion, and this makes it possible to obtain an expression for the effective cross section in the form of a correct asymptotic expansion in powers of Z^{-1}.[49,50] The structure of the result reflects both excitation possibilities (11a) and (11b), as well as the presence of the process (12) that competes with (11b).

We designate the complete set of quantum numbers of the channel by $\Gamma = \langle \gamma l \Gamma_T \rangle$, where γ characterizes the state of the ion, l is the orbital angular momentum of the incident electron, and Γ_T contains the total angular momenta and other quantum numbers characterizing the type of coupling. The total cross section of the transition $\gamma_0 \to \gamma_1$, expressed in units of πa_0^2 (a_0 is the Bohr radius), is equal to

$$\sigma(\gamma_0 \to \gamma_1) = \sum_{l_0 l_1 \Gamma_T} \sigma(\gamma_0 l_0 \to \gamma_1 l_1), \tag{13}$$

where the partial cross sections $\sigma(\gamma_0 l_0 \to \gamma_1 l_1)$, averaged over the resonances, consist of two parts:

$$\sigma(\gamma_0 l_0 \to \gamma_1 l_1) = \frac{g(\Gamma_1)}{g_0(\gamma_0) Z^4 E} \left(|T^p_{\Gamma_0\Gamma_1}|^2 + |T^r_{\Gamma_0\Gamma_1}|^2 \right) + O\left(\frac{1}{Z^6}\right); \tag{14}$$

Here $g(\gamma_0)$ and $g(\Gamma_1)$ are the statistical weights of the initial state and of the channel Γ_1, while E is the energy of the incident electron, expressed in Coulomb units. $T_{\Gamma_0\Gamma_1}$ are the elements of the transition matrix which is connected with the scattering matrix S by the relation $S = 1 + 2iZ^{-1}T$. The T-matrix element that determines the potential scattering, $T^p_{\Gamma_0\Gamma_1}$, should be calculated in first-order perturbation theory (the so-called Born–Coulomb theory) with exchange taken into account.

The resonant part is equal to

$$\begin{gathered} |T^r_{\Gamma_0\Gamma_1}|^2 = \frac{1}{2} \sum_c w_{c\Gamma_0} \frac{A_a(c \to \Gamma_1)}{A_a(c) + A_r(c)} [1 - \theta(E - \Delta E_{c\Gamma_0})], \\ \theta(x) = 1, \quad x > 0, \quad \theta(x) = -1, \quad x < 0, \end{gathered} \tag{15}$$

where the summation is over all the energywise closed channels, $w_c\Gamma_0$ is the probability of electron capture into resonant states $c = \{\gamma l\}$, $A_a(c \to \Gamma_1)$ is the probability of autoionization decay with formation of a final (excited) state Γ_1, while $A_a(c)$ and $A_r(c)$ are the total probabilities of the autoionization and radiative decays of the resonance state. The step function θ indicates that the resonant contribution is given by the energywise closed channels and vanishes when these channels are opened.

In formulas (14) and (15), the dependence of the ion charge Z has been separated in explicit form. Thus, for multiply-charged ions ($Z \gg 1$) the accuracy with which the cross sections are calculated can be characterized by the expression

$$\frac{\Delta\sigma}{\sigma} \sim \frac{1}{Z^2}. \tag{16}$$

The results of a calculation with the aid of formulas (13–15) are shown in Fig. 2 for two transitions in the lithium-like ion of oxygen O VI.[50] For the transition

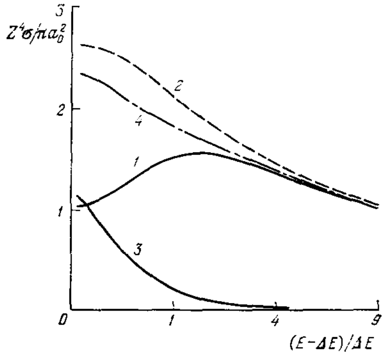

FIG. 3. Cross sections for the excitation of the transition $1s^2 \rightarrow 1s2p$ in the O VII ion.[51] 1—for the 2^1P level with exchange taken into account, 2—the same without allowance for exchange, 3—for the 2^3P level with allowance for exchange, 4—some of cross sections 1 and 3.

$1s^22p \rightarrow 1s^23s$ the effect of the resonance scattering determines the order of magnitude of the cross section at incident-electron energy values from the threshold 67.4 eV to $E \approx 100$ eV. This situation is realized in cases when there exist effectively excited levels whose excitation thresholds exceed the thresholds of the investigated transition. By way of example we can indicate optically forbidden transitions between fine-structure components and principal configurations of the type $2s^22p^k$, which are of interest to astrophysical applications. In other cases, the contribution of the resonance scattering is not so large, and, for example, this results in a correction $\lesssim 30\%$ to the cross section for the excitation of intercombination transition $1s^2(^1S) \rightarrow 1s2p(^3P)$ in helium-like ions.

Another factor that directly influences the magnitude of the cross section, or more accurately of its potential part, is the exchange effect. In the case $Z \gg 1$ (which corresponds in practice to the condition $Z > 5$), the potential part of the scattering should be calculated in the Born–Coulomb approximation with allowance for exchange. Such a calculation,[51] based on the method of orthogonalized functions,[52] shows that in the case of excitation of resonant and other singlet levels in He-like ions the cross section in the near-threshold region is half as large as without allowance for exchange. This conclusion is valid for all values $Z > 5$. The results of the calculation are shown in Fig. 3.

Summarizing the foregoing, we must note the following. The exchange effect is important when the excitation energy is close to the ionization potential. A typical example is excitation of H- and He-like ions from the ground state. Resonant excitation yields in this case relatively small corrections to the potential excitation. In the opposite limiting case, when the excitation energy is much less than the ionization potential (e.g., for Li- and Be-like ions), the exchange is insignificant and the potential cross section is determined by the Born–Coulomb approximation. In this case, however, the contribution of the resonant excitation is large and must be taken into account.

Applications call for the knowledge of the excitation rates, i.e., the cross sections (13) averaged over the Maxwellian distribution of the electrons. For each partial cross section (14), this averaging can be carried out analytically, after which the results of (13) can be represented in the form of a two-parameter formula.[53] The rate of excitation of the transition $0 \rightarrow 1$ is

$$C_{01} = \langle v\sigma_{01}\rangle = 10^{-8}\left(\frac{E_1}{E_0}\frac{\mathrm{Ry}}{\Delta E_{01}}\right)^{3/2}\frac{B}{g_0}e^{-\beta}\beta^{1/2}\frac{\beta+\delta_{S_0S_1}}{\beta+X}\,(\mathrm{cm}^3/\mathrm{sec}),$$
$$\beta = \frac{\Delta E_{01}}{kT}, \qquad \Delta E_{01} = E_1 - E_0, \tag{17}$$

Here E_0 and E_1 are the energies of the levels 0 and 1, reckoned from the boundary of the continuous spectrum, Ry = 13.6 eV, and g_0 is the statistical weight of the initial state. The parameters B and X depend on the type of the transition and do not depend, in accordance with (14), on the charge Z. Their values for the cases of greatest importance in the applications are given in Table VI (see also[54]).

Expression (17) has a simple structure and describes both limiting cases of low ($\beta \gg 1$) and high ($\beta \ll 1$) temperatures. Since the cross section for the excitation of the ion is finite at the threshold, it follows that at $\beta \gg 1$ the averaging over the Maxwellian distribution yields $C_{01} = \mathrm{const}\,\beta^{1/2}e^{-\beta}$. In the opposite limiting case $\beta \ll 1$, the main contribution to the integral is made by the part of the cross section that is asymptotic in the energy. It is necessary then to take into account the fact that the cross sections of the intercombination transitions ($|S_0 - S_1| = 1$) decrease in proportion to E^{-3}, whereas the cross section for the transitions between levels having the same spin ($S_0 = S_1$) have a dependence like E^{-1} (or like $E^{-1}\ln E$ for optically allowed transitions), and it is this which leads to the difference between the power-law dependences on β for the different types of transitions. The dependences on E_0, E_1, and E are established in similar fashion. The parameters B and X, which determine the specifics of the ion and of the transitions, can be obtained only by a numerical method.

TABLE VI. The parameters B and X for the calculation of the rates of excitation and ionization of He-like ions.[54]

Transition	B	X	Transition	B	X
$1^1S_0-2^3S_1$	3.4	0.38	$-i$	8.7	0.68
-2^3P_0	2.32	0.63	$2^3P_1-2^3P_2$	0.72	0.99
-2^3P_1	6.86	0.63	-2^1S_0	$9.3\cdot10^{-4}$	$1.2\cdot10^{-3}$
-2^3P_2	11.6	0.63	$2^3P_2-2^1P_1$	0.07	0.017
-2^1S_0	6.0	0.52	-3^3	67.2	0.50
-2^1P_1	20	0.03	-4^3	46.2	0.46
-3^3	29.6	0.70	$-i$	26.1	0.68
-3^1	43.8	0.26	$2^3P_2-2^1S_0$	$7.7\cdot10^{-4}$	$5.3\cdot10^{-4}$
-4^3	32.5	0.44	-2^1P_1	0.12	0.017
-4^1	32	0.44	-3^3	112	0.50
$-i$	16	0.62	-4^3	77	0.46
$2^2S_1-2^3P_0$	0.06	0.04	$-i$	43	0.68
-2^3P_1	0.18	0.04	$2^1S_0-2^1P_1$	0.027	0.082
-2^3P_2	0.30	0.04	-3^1	17.8	0.44
$2^3S_1-2^1S_0$	0.047	0.0092	-4^1	13.4	0.54
-2^1P_1	0.064	0.029	$-i$	10	0.99
-3^3	53.4	0.44	$2^1P_0-3^1$	67	0.50
-4^3	40	0.54	$2^1P_0-4^1$	46	0.46
$-i$	30	0.99	$-i$	26	0.63
$2^3P_0-2^3P_1$	0.14	0.87	3^3-4^3	525	0.47
-2^3P_2	0.495	0.99	$-i$	234	0.82
-2^1S_0	$3.9\cdot10^{-4}$	$1.5\cdot10^{-3}$	3^1-4^1	175	0.47
-2^1P_1	0.023	0.017	$-i$	78	0.82
-3^3	22.4	0.5	4^3-i	315	0.70
-4^3	15.4	0.46	4^1-i	105	0.70

The transition 1^1S_0–4^3 signifies a transition from the ground state to all the triplet levels with principal quantum number $n = 4$.

Their values are chosen such as to make formula (17) the best apppximation of the results of the numerical integration of the cross sections with the Maxwellian distribution in the temperature region of physical interest.

Similarly, the ionization rate of the level 0 is given by

$$C_{0i} = \langle v\sigma_{0i}\rangle = 10^{-8}\left(\frac{\mathrm{Ry}}{|E_0|}\right)^{3/2}\frac{B}{g_0}\frac{\beta^{1/2}}{\beta+X}e^{-\beta}(\mathrm{cm^3/sec}), \quad \beta = \frac{|E_0|}{kT}, \tag{18}$$

where the same notation is used and the parameters B and X are also given in Table VI.

We shall compare subsequently the theoretical results presented here with the available experimental data on the rates of excitation by electron impact.

B. Resonance lines

We consider the main characteristics of the excitation of resonance lines, using by way of illustration the transition $1s2p\,^1P_1 \to 1s^2\,^1S_0$ in He-like ions. The resonance-line intensity, defined as the product of the population of the 1^1P_1 level by the probability of its radiative decay, is equal to

$$I_R = N_{\mathrm{He}} N_e \frac{C_R}{A_R+Q_R} A_R\,(\mathrm{photon/cm^3\ sec}), \tag{19}$$

where N_e and N_{He} are the concentrations of the electrons and of the He-like ions in the ground state, C_R is the effective excitation rate, A_R is the probability of the radiative transition to the ground state, and Q_R is the rate of collision quenching of the resonant level. The factor $C_R/(A_R+Q_R)$ follows in obvious fashion from the solution of the stationary kinetic equations for the determination of the populations of the excited levels. Inasmuch as $A_R \gg Q_R$ both in a tenuous astrophysical plasma and in a dense laboratory plasma, we can rewrite (19) in the form

$$I_R = N_{\mathrm{He}} N_e C_R. \tag{20}$$

Under low-density conditions (solar corona), there are no secondary processes and the recombination population and the cascades from the higher excited states result in small corrections to the rate of the direct excitation from the ground state. In this case

$$C_R = \langle v\sigma(1s^2\,^1S_0 \to 1s2p\,^1P_1)\rangle. \tag{21}$$

With increasing electron density, the two-photon radiative decay of the metastable level $1s2s\,^1S_0 \to 1s^2\,^1S_0$ begins to be suppressed by the collision transition $1s2s\,^1S_0 \to 1s2p\,^1P_1$. The corresponding critical density

$$N'_e = \frac{A_r(1s2s\,^1S \to 1s^2\,^1S)}{\langle v\sigma(1s2s\,^1S \to 1s2p\,^1P)\rangle} \tag{22}$$

for the isoelectronic sequence of helium can be analytically approximated as follows[26]

$$N'_e \approx 7\cdot 10^5 (Z_n-1)^{9.3}\ \mathrm{cm^{-3}} \tag{23}$$

where Z_n is the charge of the nucleus. In active regions and in flares on the sun we have $N_e \ll N'_e$ and the rate of excitation of the resonance line is determined by (21). In laboratory-source plasma we have $N_e \gg N'_e$ so that in this case

$$C_R = \langle v\sigma(1s^2\,^1S \to 1s2p\,^1P)\rangle + \langle v\sigma(1s^2\,^1S \to 1s2s\,^1S)\rangle. \tag{24}$$

In astrophysical plasma, besides the resonance line one can observe with good spectroscopic resolution transitions from the triplet levels 2^3P and 2^3S. Owing to the smallness of the electron density, the electron quenching of these levels can be neglected, and the corresponding intensities are determined by formulas similar to (20)–(21). The sum of the intensity of the triplet lines referred to the intensity of the resonance lines is determined under these conditions by

$$G = \frac{I_T}{I_R} = \frac{\langle v\sigma(1s^2 \to 1s2s\,^3S)\rangle + \sum_j \langle v\sigma(1s^2 \to 1s2p\,^3P_j)\rangle}{\langle v\sigma(1s^2 \to 1s2p\,^1P)\rangle}. \tag{25}$$

The measured value of G for O VII, Ne IX, and Mg XI is close to unity (see e.g., [33,35]). The results of the theoretical methods of calculating the excitation rates, which were described in the preceding section (see formula (17) and Table VI), give good agreement with the observed values. In the interval $\beta = 5-6$, in which the emission of the indicated lines takes place, the use of the data of Table VI yields $G = 0.9-1$, which agrees with the observed values within the limits of the measurement errors.

In a laboratory plasma, the effective rate of excitation of the resonance lines of He-like ions (24) was measured by spectroscopic methods, accompanied by simultaneous independent measurements of the electron temperature and density with accuracy ±15% (see[25]). A detailed comparison[27] of the calculations discussed here with the measurements yields in the interval $\beta = 2.5-3$, a summary parameter $B = 25$ for the 2^1P and 2^1S levels, a result that deviates strongly from the data of Table VI.

The fact that the existing theory makes it possible to describe quantitatively the rates of excitation of ions by electron impacts will be used subsequently to establish the mechanisms whereby the satellites are excited and to analyze the modern methods of spectroscopic diagnostics of plasma.

C. Satellites of resonance lines

The main processes whereby autoionization states are produced and lead to the appearance of satellites of resonance lines are direct excitation of the K shells and dielectronic recombination. The latter is the process inverse to autoionization

$$A_Z(\gamma_0) + e \rightleftarrows A^{**}_{Z-1}(\gamma nl). \tag{26}$$

It is obvious that dielectronic recombination cannot lead to the formation of hydrogen-like ions in view of the impossibility of simultaneously satisfying the energy and momentum conservation laws in processes (26) in a system of two particles. Under thermodynamic-equilibrium conditions, the rate of dielectronic recombination C_d is connected with the autoionization probability A_a by the relation

$$\frac{C_d}{A_a}=\frac{g_s}{2g_0}\left(\frac{2\pi}{m}\right)^{3/2}\frac{\hbar^3}{(kT)^{3/2}}e^{-E_s/kT}. \quad (27)$$

Here g_s and g_0 are the statistical weights of the levels γnl and γ_0, respectively, E_s is the energy distance between these levels, T is the electron temperature, m is the electron mass, and k and $\hbar$ are the Boltzmann and Planck constants. Under stationary conditions, the population N_s of the autoionization level γnl is connected with the ion density N_Z and the ground state by the relation

$$N_s(A_a+\sum A_r)=N_eN_ZC_d. \quad (28)$$

for the intensity of the satellites produced in the radiative transition $\gamma nl\to\gamma' nl$ we obtain

$$I_s^d=N_sA_r=N_ZN_eC_d\frac{A_r}{A_a+\sum A_r}(\text{photon/cm}^3\text{ sec}); \quad (29)$$

Here A_r and $\sum A_r$ are the probabilities of the radiative transition via the given channel and the total probability of the radiative decay of the γnl level, respectively.

Taking (27) into account, we write down (29) in explicit form:

$$I_s^d=N_ZN_e4\pi^{3/2}a_0^3\frac{g_s}{g_0}\left(\frac{\text{Ry}}{E_s}\frac{E_s}{kT}\right)^{3/2}\frac{A_aA_r}{A_a+\sum\limits_r A_r}e^{-E_s/kT}, \quad (30)$$

where a_0 is the Bohr radius. It is important that the ratio of the intensity of the satellite produced as a result of the dielectronic recombination to the intensity of the resonance lines does not depend on the density of the electrons and ions, and is equal to

$$\frac{I_s^d}{I_R}=\frac{C_d}{C_R}\frac{A_r}{A_a+\sum A_r}, \quad (31)$$

where C_R is the rate of excitation of the resonance line and is determined by expressions (21) and (24) for tenuous and dense plasmas, respectively. Using (17) and putting $\beta\gg 2.5$ (corresponding to temperatures for which emission of the indicated lines takes place), we obtain

$$i_s^d=\frac{I_s^d}{I_R}=1.5\cdot 10^{-15}\frac{g_s}{g_0}\frac{A_a}{B}\frac{A_r}{A_a+\sum A_r}n^2ye^y,\qquad y=\frac{|E_0|}{(n^2kT)}. \quad (32)$$

Thus, the relative intensity of the dielectronic satellites can be used to determine the temperature, provided that the probabilities of the autoionization and radiative decay are calculated with good accuracy.

By now, systematic calculations of the values of A_a and A_r have been made on the basis of the Hartree–Fock[26,27] and Coulomb[36,39] approaches described in Sec. 1. Just as in the case of the calculation of the wave lengths, both calculation methods lead to a good quantitative agreement between the results. The values of A_a and A_r, which make it possible to calculate the ratio (32), are listed in Table V for a number of multiply-charged ions that are of astrophysical interest and are investigated under laboratory conditions.

Another satellite-formation mechanism is the excitation of K-shell electrons by direct electron impact. This process is not very effective for He-like ions, since the probability of simultaneously exciting two electrons is low in comparison with single-electron excitation. For this reason, the satellites of the resonance lines of H-like ions are predominantly of recombination origin. For ions with three (and more) electrons, excitation of the K shell by electron impact can make an appreciable contribution to the formation of autoionization levels, which in many cases can predominate over the dielectron recombination. In order not to introduce a cumbersome notation, we consider this process with Li-like A_{Z-1} ions as an example. The excitation of an electron from the K shell

$$A_{Z-1}(1s^22l)+e\to A_{Z-1}^{**}(1s2l2l')+e \quad (33)$$

leads to a satellite intensity

$$I_s^K=N_{Z-1}N_e\langle v\sigma_s\rangle\frac{A_r}{A_a+\sum A_r}(\text{photon/cm}^3\text{ sec}). \quad (34)$$

The relative intensity is in this case also independent of the electron density

$$i_s^K=\frac{I_s^K}{I_R}=\frac{N_{Z-1}}{N_Z}\frac{\langle v\sigma_s\rangle}{\langle v\sigma_R\rangle}\frac{A_r}{A_a+\sum A_r}. \quad (35)$$

In our case, N_Z is the concentration of the He-like ions and $\langle v\sigma_R\rangle$ is the effective rate of excitation of the resonance line; N_{Z-1} is the concentration of Li-like ions in the corresponding lower states ($1s^22s$ or $1s^22p$), depending on which of the satellites is considered; $\langle v\sigma_s\rangle$ is the excitation rate.

At low electron density, the configuration $1s^22p$ is practically unpopulated. With increasing electron density, a Boltzmann distribution is established between the $1s^22s$ and $1s^22p$ configurations.

The corresponding critical density

$$N_e''=\frac{A_r(1s^22p\to 1s^22s)}{\langle v\sigma(1s^22s\to 1s^22p)\rangle} \quad (36)$$

can be approximated at[26]

$$N_e''\approx 6\cdot 10^{12}(Z_n-2)^{4,3}\text{ cm}^{-3}. \quad (37)$$

Just as in the previously discussed case (23), in plasma of astrophysical objects we have $N_e\ll N_e''$, whereas under laboratory conditions we have in most cases $N_e\gg N_e''$.

In the calculation of the effective excitation cross sections (33) it is necessary to take into account, besides the already indicated exchange and resonant-excitation effects, also the presence of equivalent electrons in the initial and final channels of the reaction, which lead to the need for a correct utilization of the technique of adding angular momenta. Let us illustrate this with a very simple example. The excitation cross section of the transition

$$1s^2\,(^1S)\,2s\,^2S\to 1s\,\{2s^2\,(^1S)\}\,^2S \quad (38)$$

in an Li-like ion is equal to half the cross section of the $1s^2-1s2s\,^1S$ transition in an He-like ion with the same nuclear charge. The explanation is that the configuration $1s\,\{2s^2(^3S)\}\,^2S$ does not exist: two equivalent s electrons cannot have parallel spins. The general formulas for the cross sections and the numerical cal-

TABLE VII. Relative intensities of satellites produced effectively upon excitation of the K shell by electron impact, expressed in the form

$$i_s^K(T_Z)=i_s^K(T_m)\,\Phi\left(\frac{T_Z}{T_m}\right),\quad \Phi(1)=1,$$

where T_m is the temperature corresponding to the maximum emission intensity of the resonance line of an He-like ion.

a) Values of $i_s^K(T_m)$[27] at a density $N_e > N_e''$ (36).

	Mg	Ca	Fe		Mg	Ca	Fe
a	0.0022	0.0102	0.0104	r	0.0003	0.0009	0.0008
d	0.0008	0.0028	0.0042	t	—	0.0018	0.0074
m	0.0001	0.0019	0.0058	u	0.0002	0.0010	0.0011
q	0.0015	0.0097	0.0238	v	0.0001	0.0006	0.0010

b) Values of $\Phi(T_Z/T_m)$[27]

T_Z/T_m	Mg	Ca	Fe	T_Z/T_m	Mg	Ca	Fe
0.123	92.0	77.5	75.5	1.30	0.945	0.811	0.551
0.159	35.5	34.5	35.2	1.69	0.875	0.609	0.365
0.207	8.75	12.95	12.68	2.20	0.782	0.441	0.251
0.269	3.15	6.18	6.62	2.86	0.664	0.381	0.165
0.350	1.58	3.82	4.01	3.71	0.541	0.228	0.115
0.455	1.16	2.77	2.81	4.83	0.450	0.161	0.081
0.592	1.07	2.21	2.09	T_m (10^6 °K)	6.02	25.4	52.8
0.769	1.04	1.67	1.52	N_{Li}/N_{He}			
1.00	1.00	1.00	1.00	at $T_Z=T_m$	0.012	0.043	0.079

culations of the excitation rates (23) are given in[27]. As we shall see subsequently, one of the criteria of the good accuracy of these calculations is the quantitative agreement between the calculated intensities (35) and those observed in laboratory and astrophysical experiments.

We note that the ratio $\langle v\sigma_s\rangle/\langle v\sigma_R\rangle$ is practically independent of the electron temperature, inasmuch as the excitation energies of the resonant levels and of the satellites are close.

In an equilibrium plasma, the concentration ratio N_{Z-1}/N_Z is determined by the electron temperature T and is obtained from the condition that the ionization and recombination processes be equal:

$$N_{Z-1}N_eC_{Z-1}^i=N_ZN_eR_Z; \tag{39}$$

Here C_{Z-1}^i is the combined rate of all the processes of the ionization of the ion A_{Z-1}, while R_Z is the combined rate of all the processes of recombination with formation of the ion A_{Z-1}. The system (39) contains their total number, equal to the number of electrons in the neutral atom. Its solution can be written in elementary form. Putting

$$p_Z=\frac{C_Z^i}{R_Z},\quad n_Z=\frac{N_Z}{\sum\limits_j N_j}, \tag{40}$$

we get

$$n_Z=\Big(\prod_{j=0}^{Z-1}p_j\Big)\Big/\Big(\sum_j\prod_{k=0}^{j-1}p_k\Big),\qquad p_0=1. \tag{41}$$

In the low-temperature plasma containing multiply-charged ions (both astrophysical and laboratory plasma), the process of thermodynamically reversible ionization by electron impact—three-particle recombination—makes a negligibly small contribution in comparison with the binary recombination processes. Therefore in the calculation of R_Z we can confine ourselves to the combined rate, over all the levels of the photorecombination and the dielectronic recombination. In the calculation of C_Z^i, besides the rate of ionization from the ground state, it is necessary to take into account the rate of excitation of the autoionization levels. Calculations of this kind were performed for the elements from H to Ni in the temperature region 10^6–10^8 °K independently in[56,57] and in[58,59]. Their results are in good agreement.

The relative intensity i_s^d is determined directly from formula (32) using the values of A_r and A_a from Table V. The intensities i_s^K (35) are given in Table VII. We note that for a number of lines we have $i^d \gg i^K$, whereas for others the inequality is reversed. Finally, in a large number of cases $i^d \approx i^K$.

Thus, a comparison of the calculated relative intensities with the measured ones allows us to access the accuracy of the calculation of the rates of the electron-ion processes concerned here. On the other hand, when the employed theoretical methods are sufficiently reliable, we are justified also in formulating the inverse problem, namely the determination of the parameters of a high-temperature plasma from the relative intensities of the spectral lines.

4. SPECTROSCOPIC DIAGNOSTICS OF HIGH-TEMPERATURE PLASMA

We begin the analysis with a Maxwellian distribution of the electron velocities. There is direct experimental evidence[60–62] indicating that in a number of cases the electron distribution in a laser plasma deviates from Maxwellian, and this leads to the appearance of a certain number (less than 1%) of fast electrons; this phenomenon has also been theoretically explained.[63,64] However, the intensities of the spectral lines considered above are altered thereby by not more than several percent, as follows from elementary estimates of the rates of excitation and dielectronic recombination. Thus, although a small fraction of the fast particles can lead to noticeable effects in the hard component of the continuous x-ray spectrum,[62] its contribution to the line intensity can be neglected.

More significant is the assumption that the degree of ionization of the plasma corresponds to the electron temperature, an assumption extensively used in spectroscopy until recently. This assumption, however, contradicts the experimental data. Frequently the time of existence (and observation) of a laboratory plasma is shorter than the characteristic time in which ionization equilibrium is established, the latter being of the order of $\tau \propto (C_Z^i+R_Z)^{-1}N_e^{-1}$ sec. Actually, an analysis of the spectra can be carried out without using the indicated assumption and it is possible moreover to establish whether the observed plasma is ionizing, in equilibrium, or recombining.[26,27]

We shall determine the plasma parameters comparing the theoretical calculations of the relative intensities with the experimental ones obtained with good spectroscopic resolutions. As already noted earlier,

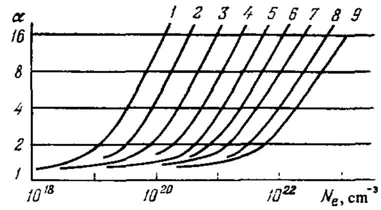

FIG. 4. Dependence of α on N_e in a dense plasma.[54] 1—Na X; 2—Mg XI, 3—Al XII, 4—Si XIII, 5—P XIV, 6—S XV, 7—Cl XVI, 8—Ar XVII, 9—K XVIII.

a number of satellites are excited only on account of dielectronic recombination (the satellites of the resonance lines of H-like ions, the j and k satellites of resonance lines of He-like ions, etc.). In this case formula (32) enables us to reconstruct the electron temperature T from one satellite (or from several).

For satellites that are produced exclusively by excitation of K shells (for example q), formula (35) allows us to reconstruct the ion concentration ratio N_{Z-1}/N_Z. We shall assume that this ratio

$$\frac{N_{Z-1}}{N_Z} = f(T_Z) \tag{42}$$

is a function of the parameter T_Z, defined as the temperature at which a given value N_{Z-1}/N_Z would exist in the equilibrium plasma. Then $T_Z = T$ signifies an equilibrium plasma, $T_Z < T$ corresponds to an ionizing plasma, and $T_Z > T$ to a recombining plasma. A check on the validity of the obtained values of T and T_Z is the description of the intensities of the remaining satellites produced as a result of both mechanisms, without any additional assumptions.

The relative intensities of the satellites do not depend on the electron density, so that it is possible to use the same methods to determine T and T_Z in an astrophysical and in a laboratory plasma. At the same time, the problem of measuring the electron density in a laboratory plasma is most urgent. Its solution can be obtained by investigating the relative intensities of the intercombination lines of He-like ions.[19,54,56] Consider the ratio

$$\alpha = \frac{N(2\,^1P)\,A_r(2\,^1P \to 1\,^1S)}{N(2\,^3P_1)\,A_r(2\,^3P_1 \to 1\,^1S)}, \tag{43}$$

where N stands for the populations of the resonant and intercombination levels, as a function of the electron density. At $N_e \ll N'$ (23) the probabilities of all the collision transitions are much lower than the radiative probabilities, and the conditions of the solar corona are realized. Then α does not depend on the plasma density and is equal to the ratio of the excitation rates of the levels 2^1P and 2^3P_1 from the ground state by electron impact (c.f. (25)). At $N_e \gtrsim N_e'$ the rate of excitation of the resonance line is determined by formula (24), and the probabilities of the radiative decay of the triplet levels 2^3S and 2^3P_2 become successively smaller than the probabilities of the collision transition between the triplet levels. All the triplet levels then begin to become de-excited via the transition $2^3P_1 - 1^1S$, and the ratio α should decrease to the value

$$\alpha_0 = \frac{\langle v\sigma(1\,^1S \to 2\,^1P)\rangle + \langle v\sigma(1\,^1S \to 2\,^1S)\rangle}{\langle v\sigma(1\,^1S \to 2\,^3S)\rangle + \sum_{j=0}^{2} \langle v\sigma(1\,^1S \to 2\,^3P_j)\rangle}, \tag{44}$$

which is approximately 20% larger than G^{-1} (25).

With further increase of N_e, the triplet levels become depleted as a result of ionization by electron impact and as a result of transfer of excitation to the singlets, and this leads to a sharp increase of α. The dependence of α on N_e in first-order approximations can be obtained by assuming that there is a Boltzmann equilibrium between the levels 2^3P_j and 2^3S, and if account is taken of the following processes: radiative decay of the levels 2^1P_1 and 2^3P_1, the collision transitions $2^1S - 2^1P_j 2^3L_j \rightleftarrows 2^1L$, and the ionization of the triplet levels.

The expression for α then takes the form[54,65]

$$\alpha = \alpha_0 + N_e\,[(\alpha_0 + 1)\,C_{t_s} + \alpha_0 C_{t_i}]\,[0.25 A_r\,(2\,^3P_1 - 1\,^1S)]^{-1}, \tag{45}$$

where α_0 is given by (44). Here C_{t_s} and C_{t_i} are the rates of excitation transfer and ionization from the triplets, averaged over the triplet states.

The linear dependence of α on N_e in this region turns out to be quite convenient for the determination of the electron density. Numerical solution of the system of balance equations for the determination of the populations with allowance for cascades from levels $n > 2$[54] leads to small deviations from the results given by (45). The values of the parameter α as a function of N_e are given in Fig. 4.

A characteristic feature of the diagnostic methods discussed here is the simultaneous measurement of the electron temperature T of the ionization state T_Z, and of the electron density by using closely-lying lines of the same ions, so that the obtained value of the parameters can be related to a single spatial region. It is then unnecessary to perform absolute measurements of the intensities and the measurement time can be

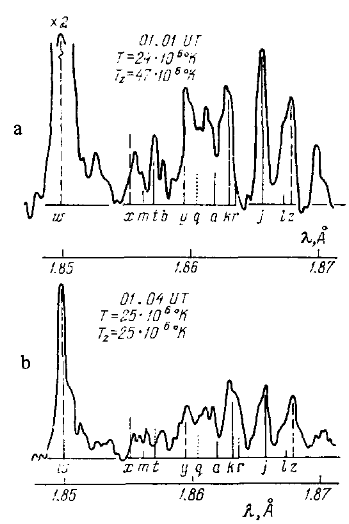

FIG. 5. Comparison of the spectra of the iron ions Fe XXV–Fe XXIV, registered in a solar flare,[1–3] with the calculations of[27].

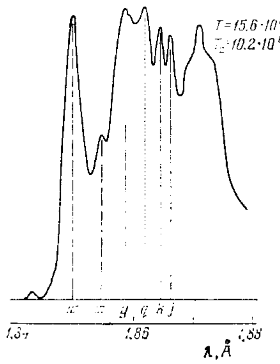

Fig. 6. Comparison of the spectrum of the ions Fe XXV–Fe XXIV registered in a solar flare, [4] with the calculated spectrum.

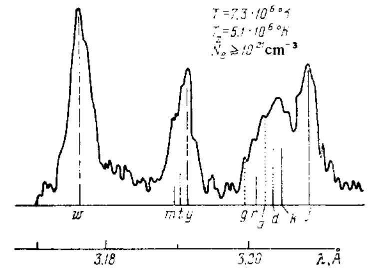

FIG. 8. Comparison of the experimental spectrum of the ions Ca XIX–Ca XVII, obtained with the aid of a laser plasma, [10] with the calculated spectrum.

shorter than the characteristic time required to establish the ionization equilibrium.

5. COMPARISON OF THE CALCULATIONS WITH THE EXPERIMENTAL DATA

At the present time there are many published experimental spectra obtained with good spectroscopic resolution under laboratory and astrophysical conditions. A comparison of the theoretical and experimental results yields additional criteria for the accuracy of the existing calculations and demonstrates the volume of information obtainable by spectroscopic methods. The results are given in Figs. 5–9. The solid curves represent the experimental spectra, and the vertical lines represent the theoretically calculated intensities. The resonance and intercombination lines of He-like ions are shown dashed. The contribution to the satellite intensity from the dielectronic recombination is shown by solid segments, while the contribution from the excitation of the K shell is shown by dotted segments. The designations of the lines in the figures correspond to Table III. The relative intensities i_s^d were calculated by formula (32) in conjunction with Table V. The values of i_s^K are given directly in Table VII in accordance with[27].

A. X-ray flares on the sun

The spectra of He-like iron ions Fe XXV and the satellites of the resonance lines measured by the Li-like ions Fe XXIV are observed in the solar corona only during the time of x-ray flares. Figure 5 shows two spectra registered during the course of a flare of class 2B (November 16, 1970) on board the satellite "Interkosmos-4" with an interval of 3 min.[1–3] From a comparison of the observed intensities with those calculated in[27] it is seen that the main mechanism of satellite formation is dielectronic recombination, and in the initial state (Fig. 5a) the plasma deviated strongly from equilibrium: T_z was double T. In accordance with the conclusions of the preceding section, such a relation between T and T_z corresponds to a recombining plasma, as is indeed confirmed by the spectrum on Fig. 5b, where $T_z = T$. The measured wave lengths on the whole agree with the calculated ones. A noticeable exception is the intercombination line x. Its deviation from the calculated position is attributed to an error in the measurement, as confirmed by the experimental spectrum (see Fig. 6) obtained by the same authors[4] on board the "Interkosmos-7" (August 4, 1972). Good agreement is observed here between experiment and theory in the values of the wave lengths of all the lines. The high intensity of all the satellites indicates a colder plasma, and the large intensity of the q line, which is produced exclusively as a result of excitation of the K shell in Li-like ions, points to a high relative concentration of the Li-like ions corresponding an "underionized" plasma ($T_z < T$). If the electron temperature remains at its previous level, in the course of time such a plasma should approach the ionization equilibrium $T_z \to T$.

B. Laser plasma

A laser plasma is characterized by a high density and a short lifetime. At the same time, the reproducibility of the x-ray spectra obtained with the aid of a

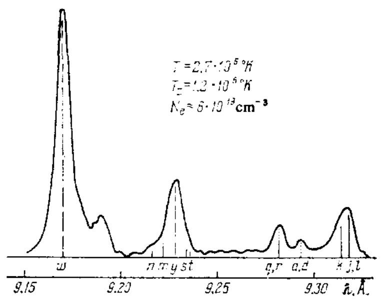

FIG. 7. Comparison of the experimental spectrum of the ions Mg XI–Mg X, obtained with the aid of laser plasma, [10] with the calculated spectrum.

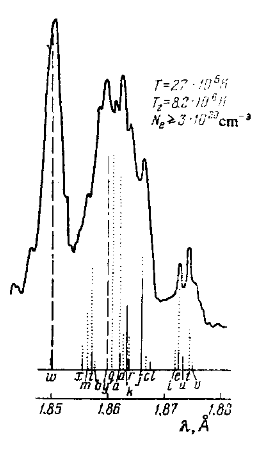

FIG. 9. Comparison of the spectrum of the iron ions Fe XXV–Fe XXIV, obtained under laboratory conditions, [24] with the calculated spectrum. [27]

laser plasma, and the spectral resolution and accuracy of wave length measurement attainable thereby, permit a sufficiently detailed identification of the lines and a determination of the parameters of such a plasma. This is illustrated in Figs. 7 and 8, which show the experimental spectra of the ions Mg XI and Ca XIX[10] in comparison with the calculated ones. The good agreement between the positions and the intensities of the lines allows us to conclude with assurance that the reconstructed parameters T and T_Z are correct. The situation $T_Z \lesssim T$ is altogether typical of a dense laser plasma, or more accurately of that plasma region which radiates in the given spectral band during the registration time, and this explains the relatively high intensity of the satellites due to excitation of the K shells. The electron density is reconstructed from the intensity of the intercombination line y in accordance with formula (45) and with more detailed calculations.[54]

C. Other laboratory sources

The spectra of iron ions in the region of the emission of the resonance lines of He-like and H-like ions are of interest in connection with investigations of the sun and of other astrophysical objects. The largest multiplicity ion obtained at present time with the aid of a laser plasma is the helium-like vanadium ion V XXII. Higher degrees of ionization were registered in experiments with installations of the low-inductance vacuum spark type.[21–24] Although in such sources the dimensions of the hot region, just as in the case of a laser plasma, are quite small, its dispersement in space from flash to flash greatly hinders high-resolution registration of the spectra. Nonetheless, this difficult experimental problem was solved, and the best of the published laboratory spectra of the iron ion[24] is shown in Fig. 9. The high intensity of the satellites produced by excitation of the K shells points to a low degree of ionization ($T_Z = 8.2\times10^6\,°\mathrm{K}$), whereas the electron temperature ($T = 27\times10^6\,°\mathrm{K}$) is approximately equal to the temperature of the x-ray flare (see Fig. 5). The reconstructed value of the electron density corresponds to the density characteristic of sources of this type, and makes it possible to refine somewhat the estimate given by the authors of the experiment.[24]

6. CONCLUSION

The foregoing review shows that methods of modern x-ray spectroscopy of high-temperature plasma are quite effective both in the investigation of the sun and under laboratory conditions. The main progress in this direction was the result of the appearance of unique possibilities of investigating astrophysical plasma with the aid of artificial earth satellites and the development of new laboratory sources of hot plasma, with simultaneous development of theoretical spectroscopy and the physics of atomic collisions.

A characteristic feature of x-ray spectrscopy is the study of the radiative decay of autoionization states of multiply-charged ions—satellites of resonance lines. Their presence concentrates the information on ions of different multiplicity in narrow spectral intervals, thereby simplifying the solution of a number of experimental problems (e.g., the technically complicated task of calibrating radiation receivers), and permits the simultaneous reference of the obtained values of the plasma parameters to a single spatial region. It is important that to reconstruct the electron temperature and the density and distribution of the ions from the degree of ionization in a nonequilibrium plasma all that are necessary are measurements of the relative intensity of a number of closely lying lines.

The presently available experimental data and their theoretical interpretation offer evidence that a number of plasma characteristics of active regions and flares on the sun (the electron temperature, the deviations from ionization equilibrium) can be successfully duplicated under laboratory conditions. Further progress in this direction is connected primarily with the development of the technique of spatial and temporal resolution in the registration of the spectra. This would make it possible, in particular, to study various stages of the development of solar x-ray flares, and to organize task-oriented experiments on their simulation.

Considerable interest can attach also to spectroscopic investigations of the dynamics of the development of laboratory plasma (both for laser plasma and for plasma of other sources). One can expect here that in earlier stages of the ionization the main contribution to the formation of the spectra will be made by direct excitation of the internal shells.

The author is indebted to L. A. Vaǐnshteǐn and B. M. Smirnov for a discussion and for useful remarks.

[1] Yu. I. Grineva, V. I. Karev, V. V. Korneev, V. V. Krutov, S. L. Mandelstam, L. A. Vaǐnshteǐn, B. N. Vasiljev, and I. A. Zhitnik, in: Proc. of 16th COSPAR (Seattle, USA), 1971, p. 243.; in: Space Research-XII, Berlin, Akademie-Verlag, 1972, p. 1553.

[2] B. N. Vasil'ev, Yu. I. Grineva, I. A. Zhitnik, V. I. Karev, V. V. Korneev, V. V. Krutov, and S. L. Mandel'shtam, Kratk. Soobshch. Fiz. 3, 29 (1972).

[3] Yu. I. Grineva, V. I. Karev, V. V. Korneev, V. V. Krutov, S. L. Mandelstam, L. A. Vaǐnshteǐn, B. N. Vasiljev, and I. A. Zhitnik, Solar Phys. 29, 441 (1973).

[4] Yu. I. Grineva, V. I. Karev, V. V. Korneev, V. V. Krutov, S. L. Mandelstam, U. I. Safronova, A. M. Urnov, L. A. Vaǐnshteǐn, B. N. Vasiljev, and I. A. Zhitnik, in: Space Research-XIV, Berlin, Akademie-Verlag, 1974, p. 453.

[5] E. V. Aglitskiǐ, V. A. Boǐko, S. M. Zakharov, G. V. Sklizkov, and A. N. Federov, Kr. Soobshch. Fiz. 12, 36 (1971).

[6] E. V. Aglitskiǐ, V. A. Boǐko, L. A. Vaǐnshteǐn, S. M. Zakharov, O. N. Krokhin, and G. V. Sklizkov, Opt. Spectrosc. 35, 963 (1973).

[7] E. V. Aglitskiǐ, V. A. Boǐko, L. A. Vaǐnshteǐn, S. M. Zakharov, O. N. Krokhin, V. S. Sklizkov, and U. I. Safronova, Preprint Fiz. Inst. Akad. Nauk SSSR, No. 112, Moscow, 1973.

[8] E. V. Aglitskiǐ, V. A. Boǐko, S. M. Zakharov, S. A. Pikuz, and A. Ya. Faenov, Kratk. Soobshch. Fiz. 12, 12 (1973).

[9] V. A. Boǐko, O. N. Krokhin, S. A. Pikuz, and A. Ya. Faenov, Pis'ma Zh. Eksp. Teor. Fiz. 20, 115 (1974) [JETP Lett. 20, 50 (1974)].

[10] V. A. Boǐko, O. N. Krokhin, S. A. Pikuz, and A. Ya. Faenov, Kvant. Elektron. (Moscow) 1, 1007 (1974) [Sov. J.

Quant. Electron. 4, 547 (1974)].
[11]E. V. Aglitskiĭ, V. A. Boĭko, O. N. Krokhin, S. A. Pikuz, and A. Ya. Faenov, *ibid.*, p. 2067 [1152].
[12]E. V. Aglitskiĭ, V. A. Boĭko, S. M. Zakharov, S. A. Pikuz, and A. Ya. Faenov, Pis'ma Ah. Eksp. Teor. Fiz. 19, 16 (1974) [JETP Lett. 19, 8 (1974)].
[13]B. J. Mallozzi, H. M. Epstein, R. G. Jung, D. C. Applebaum, B. P. Fairanal, and W. J. Gallagher, in: Fundamental and Applied Laser Physics, Ed. M. B. Feld, A. Javan and N. Kurnit, N.Y., Wiley-Interscience, 1973, p. 165.
[14]N. J. Peacock, M. G. Hobby, and M. Galanti, J. Phys. B6, L298 (1973).
[15]D. J. Nagel, P. G. Burkhalter, C. M. Dozier, J. F. Holfrichter, B. M. Klein, J. M. McMahon, J. A. Stamper, and R. R. Whitlock, Phys. Rev. Lett. 33, 743 (1974).
[16]U. Feldman, G. A. Doschek, D. J. Nagel, W. E. Behring, and D. R. Cowan, Astrophys. J. 187, 417 (1974).
[17]U. Feldman, G. A. Doschek, D. J. Nagel, D. R. Cowan, and R. R. Whitlock, *ibid.* 192, 213 (1974).
[18]P. G. Burkhalter, D. J. Nagel. and R. D. Cowan, Phys. Rev. A111, 782 (1975).
[19]E. V. Aglitskiĭ, V. A. Boĭko, A. V. Vinogradov, and E. A. Yukov, Kvant. Elektron. (Moscow) 1, 579 (1974) [Sov. J. Quant. Electron. 4, 322 (1974)].
[20]G. V. Peregudov, E. N. Ragozin, and V. A. Chirkov, ibid. 2, 1851 (1975) [5, 1018].
[21]J. L. Schwob, and B. S. Fraenkel, Phys. Letts A40, 81 (1972).
[22]J. L. Schwob, and B. S. Fraenkel, Space Sci. Rev. 13, 589 (1972).
[23]I. I. Turechek, and H. J. Kunze, Zs. Phys. A273, 111 (1975).
[24]E. Ya. Gol'ts, I. A. Zhitnik, E. Ya. Kononov, S. L. Mandel'shtam, and Yu. I. Sidel'nikov, Dokl. Akad. Nauk SSSR 220, 560 (1975) [Sov. Phys. Dokl. 20, 49].
[25]A. H. Gabriel, and T. M. Paget, J. Phys. B5, 673 (1972).
[26]A. H. Gabriel, Mont. Not. RAS 160, 99 (1972).
[27]C. P. Bhalla, A. H. Gabriel, and L. P. Presnyakov, *ibid.* 172, 359 (1975).
[28]B. Edlen and F. Tyren, Nature 143, 940 (1939).
[29]H. Flemberg, Ark. Mat., Astro., Fys. A28 (18), 1 (1942).
[30]A. H. Gabriel and C. Jordon, Nature 221, 947 (1969).
[31]N. J. Peacock, R. J. Speer, and M. G. Hobby, J. Phys. B2, 798 (1969).
[32]J. H. Parkinson, Nature 233, 44 (1971).
[33]A. B. C. Walker and H. R. Rugge, Astrophys. J. 164, 181 (1971).
[34]J. F. Meekins, G. A. Doschek, H. Friedman, T. A. Chubb, and R. W. Kreplin, Solar Phys. 13, 198 (1970).
[35]W. M. Neupert, *ibid.* 18, 474 (1971).
[36]L. A. Vaĭnshteĭn, and U. I. Safronova, Kratk. Soobshch. Fiz. 3, 40 (1972).
[37]L. A. Vaĭnshteĭn and U. I. Safronova, Astron. Zh. 48, 223 (1971) [Sov. Astron. 15, 175 (1971)].
[38]E. P. Ivanova and U. I. Safronova, J. Phys. B8, 1591 (1975).
[39]L. A. Vaĭnshteĭn and U. I. Safronova, Preprint Is. Akad. Nauk SSSR, No. 6, Moscow, 1975.
[40]C. W. F. Drake and A. Dalgarno, Phys. Rev. A1, 1325 (1970).
[41]I. D. Garsia and I. F. Mack, J. Opt. Soc. Amer. 55, 654 (1965).
[42]E. U. Condon and G. H. Shortley, Theory of Atomic Spectra, Cambridge, 1935.
[43]I. I. Sobel'man, Vvedenie v teoriyu atomnykh spektrov (Introduction to the Theory of Atomic Spectra), Fizmatgiz, 1963.
[44]A. I. Baz', Zh. Eksp. Teor. Fiz. 36, 1762 (1959) [Sov. Phys. JETP 9, 1256 (1959)].
[45]A. I. Baz', Ya. B. Zel'dovich, and A. M. Perelomov, Rassiyanie, reaktsii i raspady v nerelyativistskoĭ kvantovoĭ mekhanike (Scattering, Reactions, and Decays in Nonrelativistic Quantum Mechanics), Nauka, 1971.
[46]M. K. Gailitis, Zh. Eksp. Teor. Fiz. 44, 1974 (1963) [Sov. Phys. JETP 17, 1328 (1963)].
[47]M. J. Seaton, J. Phys. B2, 5 (1969).
[48]M. D. Hershkowitz and M. J. Seaton, J. Phys. B6, 1176 (1973).
[49]L. P. Presnyakov and A. M. Urnov, Zh. Eksp. Teor. Fiz. 68, 61 (1975) [Sov. Phys. JETP 41, 31].
[50]L. P. Presnyakov and A. M. Urnov, J. Phys. B8, 1280 (1975).
[51]L. A. Vaĭnshteĭn, Zh. Eksp. Teor. Fiz. 67, 63 (1974) [Sov. Phys. JETP 40, 32 (1975)].
[52]I. L. Beĭgman and L. A. Vaĭnshteĭn, Zh. Eksp. Teor. Fiz. 52, 185 (1967) [Sov. Phys. JETP 25, 119(1967)].
[53]L. A. Vaĭnshteĭn, I. I. Sobel'man, and E. A. Yukov, Sechenie vozbuzhdeniya atomov i ionov éleltronami (Cross Section for the Excitation of Atoms and Ions by Electrons), Nauka, 1973.
[54]A. V. Vinogradov, Yu. I. Skobelev, and E. A. Yukov, Kvant. Electron. (Moscow) 2, 1165 (1975) [Sov. J. Quant. Electron. 5, 630].
[55]A. H. Gabriel and C. Jordan, Mont. Not. RAS 145, 241 (1971).
[56]I. L. Beĭtman, L. A. Vaĭnshteĭn, and R. A. Synuyaev, Usp. Fiz. Nauk 95, 267 (1968) [Sov. Phys. Usp. 11, 411 (1969)].
[57]I. L. Beĭgman, L. A. Vaĭnshteĭn, and A. M. Urnov, Preprint Fiz. Akad. Nauk SSSR No. 28, Moscow, 1971; I. L. Beĭgman, in: Astronomiya (Astronomy), vol. 9: Itogi nauki i tekhniki (Science and Engineering Summaries) Moscow, VINITI, 1974, p. 87.
[58]C. Jordan, Mont. Not. RAS 142, 501 (1969).
[59]C. Jordan, J. Astrophys. Soc. RAS 148, 17 (1970).
[60]N. G. Basov, V. A. Boĭko, S. M. Zakharov, O. N. Krokhin, and G. V. Sklizkov, Pis'ma Zh. Eksp. Teor. Fiz. 13, 691 (1971) [JETP Lett. 13, 489 (1971)].
[61]T. W. Shearer, S. W. Mead, T. Petruzzi, F. Rainer, T. E. Swain, and C. E. Violet, Phys. Rev. A6, 764 (1972).
[62]V. A. Boĭko, O. N. Krokhin, S. A. Pikuz, A. Ya. Faenov, and A. Yu. Chugunov, Fiz. Plasmy 1, 309 (1975) [Sov. J. Plasma Phys. 1, 165].
[63]V. P. Silin, Parametricheskoe vozdeĭstvie izlucheniya bol'shoĭ moshchnosti nc plasmu (Parametric Action of High Power Radiation on a Plasma), Nauka, 1973.
[64]V. V. Pustovalov, V. P. Silin, and V. T. Tikhonchuk, Zh. Eksp. Teor. Fiz. 64, 843 (1973) [Sov. Phys. JETP 37, 429 (1973)].
[65]A. H. Gabriel and C. Jordan, in: Case Studies in Atomic Collision Physics. 2, Ed. McDaniel and McDowell, Amsterdam, North-Holland, 1972, p. 209.

Translated by J. G. Adashko